Relay-Assisted Federated Edge Learning: Performance Analysis and System Optimization

Lunyuan Chen, Lisheng Fan, Xianfu Lei, Trung Q. Duong, *Fellow, IEEE*, Arumugam Nallanathan, *Fellow, IEEE*, and George K. Karagiannidis, *Fellow, IEEE*

Abstract

In this paper, we study a relay-assisted federated edge learning (FEEL) network under latency and bandwidth constraints. In this network, N users collaboratively train a global model assisted by M intermediate relays and one edge server. We firstly propose partial aggregation and spectrum resource multiplexing at the relays in order to improve the communication of the relay-assisted FEEL system. Then, we derive analytical and asymptotic expressions of the system outage probability and convergence rate. For the purpose of improving the system performance, we further optimize the relay-assisted FEEL network by maximizing the number of users who participate in each round of federated learning, through allocation of the wireless bandwidth among users and relays. Specifically, two bandwidth allocation (BA) schemes have been proposed, assuming either instantaneous or statistical channel state information (CSI). Simulations show the advantages of the proposed BA schemes over other benchmarks, regarding the accuracy and convergence rate of the considered relay-assisted FEEL network.

Index Terms

Federated learning, edge learning, relay, outage probability, Internet of Things.

L. Chen and L. Fan are both with School of Computer Science, Guangzhou University, Guangzhou 510006, China (e-mail: 2112019037@e.gzhu.edu.cn, lsfan@gzhu.edu.cn).

X. Lei is with the School of Information Science and Technology, Institute of Mobile Communications, Southwest Jiaotong University, Chengdu 610031, China (e-mail: xflei@home.swjtu.edu.cn).

T. Q. Duong is with the School of Electronics, Electrical Engineering and Computer Science, Queens University, Belfast BT7 1NN, U.K. (e-mail: trung.q.duong@qub.ac.uk).

A. Nallanathan is with the School of Electronic Engineering and Computer Science, Queen Mary University of London, London, U.K (e-mail: a.nallanathan@qmul.ac.uk).

G. K. Karagiannidis is with Aristotle University of Thessaloniki, Greece and also with Cyber Security Systems and Applied AI Research Center, Lebanese American University (AUL), Lebanon (e-mail: geokarag@auth.gr).

I. Introduction

Recently, fast-growing applications of the Internet of Things (IoT) have generated an explosive amount of data to drive artificial intelligence (AI), widely applied in wireless communication, image processing and other fields [1]–[4]. The centralized AI applications need to aggregate distributed data from users into the server for training, which is hard to be achieved due to privacy concerns. To tackle this issue, an intelligent paradigm namely federated learning (FL) was proposed to enable multiple users to train a global model without transmitting the sensitive data [5]–[8]. In this framework, the FL server periodically selects some users as the candidates to join each round's training. Then, the selected users calculate the training loss, update the weights and transmit the local models to the server. Once they received, the server can aggregate the models and repeat the whole procedure until it converges [9]–[11].

In the same time, mobile edge computing (MEC) has become one of the most advanced technologies for reducing communication latency and energy consumption [12], [13]. For example, MEC could be used for video transmission to suppress jamming [14], where the compression parameter and power control were optimized by reinforcement learning. Besides, similar concept was used to decide offloading against jamming attacks and interference in [15], which could achieve a significant reduction in latency and energy consumption. Therefore, FL can be used in the MEC scenarios, where the mobile users perform distributed learning and transmit the trained models to be aggregated at the edge server, called federated edge learning (FEEL) [16]–[18]. The FEEL performance depends on the number of successfully participated users in the federated learning, which is however limited by the communication overhead, due to practical constraints, such as latency and bandwidth [19]–[21]. To reduce the communication overhead, a physical-layer quantization scheme was proposed to upload training models, where the compromise between FEEL performance and quantization ratio was revealed [22]. Also, to further cope with this overhead, the system resources of FEEL networks can be exploited to support more users to successfully participate into the federated learning [23], [24]. For instance, the trade-off between the communication overhead and computational capability was investigated in [25], by dividing the deep model into several sub-models, where the authors enabled heterogeneous mobile users to select models of appropriate size to reduce the amount of transmitted data. In addition, the system resources such as bandwidth can be optimized among the users, in order to meet practical requirements such as latency and energy consumption, by exploiting the channel state information (CSI) [26], [27].

Besides the above techniques, relays can be deployed in FEEL to decrease the communication overhead and thus, enhance the system communication and learning performance. In recent works, relaying has been proposed to be an effective technology in wireless communication systems to extend coverage and improve reliability without requiring additional power [28]–[30]. In the relay-assisted FEEL, some intermediate relays can be deployed to assist the communication between mobile users and the edge server. In this aspect, a FEEL network which exploits cooperative relaying with service pricing was presented in [31], where the relays only help the data communication during the model update. In addition, a relay-assisted FEEL system was investigated in [32], where multiple relays were used to improve the over-the-air computation performance. Besides assisting the data communication, the relays in the FEEL networks can help performing partial aggregation in order to reduce the total amount of data required for transmission. In this aspect, a two-tier relay-assisted FL framework was proposed in [33], where the relays assisted the model aggregation for the local gradients to achieve a partially synchronized parallel mechanism. In addition, federated learning aggregation was explored in [34] for device-to-device (D2D) communications across the wireless devices, where partial gradient aggregation was used at the relays to assist the uplink. However, so far, to the best of our knowledge, there has been little work on the relay-assisted FEEL system with limited resources, especially about the framework of performance analysis and system optimization.

In this paper, we study a relay-assisted FEEL network under latency and bandwidth constraints, where N users collaboratively train a global model assisted by one edge server and M intermediate relays. For the relay-assisted FEEL system, we propose a novel framework for the performance analysis and system optimization. Specifically, we begin with the first critical question:"*How to design a relay-assisted FEEL system that can make full use of the relays in the edge environment with limited resources?*". To answer this question, we propose to use partial aggregation and spectrum resource multiplexing at the relays to enhance the communication of the relay-assisted FEEL system. We then study the second important question: "*How to evaluate the system performance of the relay-assisted FEEL?*". To answer this question, we provide the analysis of outage probability and perform convergence analysis to reveal the impact of outage probability on the convergence rate of federated learning. Driven by the system performance analysis, we come to the third important question: "*How to optimize the FEEL performance by scheduling the system bandwidth resources?*". To answer this question, we provide instantaneous

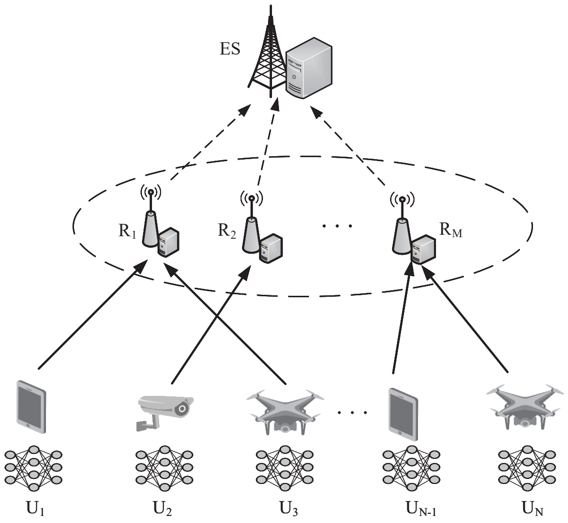

Fig. 1. Relay-assisted federated edge learning (FEEL).

and statistical bandwidth allocation (BA) schemes, which can be applicable depending on specific requirements of communication and computing scenarios. Simulation results are finally provided to illustrate the advantages of the instantaneous and statistical BA schemes.

II. Relay Assisted Federated Edge Learning

In this section, the system model of the relay-assisted FEEL network is firstly presented, and then the conventional federated learning is introduced. After that, we present the procedure for the relay selection and partial aggregation.

A. System Model

A relay-assisted FEEL network is shown in Fig. 1, where N users collaboratively train a global model assisted by one edge server ES and M intermediate decode-and-forward (DF) relays[1]. Due to severe fading, there is no direct link between the ES and users, i.e., the ES can only communicate with the users via relaying links. Besides assisting the data communication, the relays can also perform the model aggregation, in order to reduce the communication and computing overhead at the server. Let $\mathcal{U} \triangleq \{\mathrm{U}_1, \mathrm{U}_2, \dots, \mathrm{U}_N\}$ denote the set of N users, where

[1] It is straightforward to adopt the DF relaying protocol to decode and recover the model weights, in order to aggregate models at the relays in this paper. Note that this work can be extended to other relaying protocols, like AF protocol with some minor modification. In particular, we can use the summation property of wireless channels and introduce over-the-air computing technology to aggregate models without decoding and re-modulation.

device $\mathrm{U}_k \in \mathcal{U}$ has a local trainable dataset D_k and it can perform local stochastic gradient descent (SGD) on D_k. In addition, we use $\mathcal{R} \triangleq \{\mathrm{R}_1, \mathrm{R}_2, \dots, \mathrm{R}_M\}$ to denote the relay set, in which each relay can receive the local models from the N IoT users through wireless links. Then, the relays can perform partial aggregation and further transmit the aggregated models to the ES for global aggregation through wireless links. Due to the limitation in the size, each node in the system is assumed to have a single antenna.

B. Conventional Federated Learning

In the conventional FL network, multiple users with distributed data train a global model assisted by an edge server, where the intermediate relays are not involved. For such a network, the FL can be described by the following problem

$$\min_{w} F(w) = \sum_{k=1}^{N} \frac{|D_k|}{|D|} F_k(w), \tag{1}$$

where w represents the global model parameter, $|D_k|$ denotes the training sample amount in user U_k, and $|D| = \sum_{k=1}^{N} |D_k|$. Notation $F_k(w)$ is the local loss function of user U_k,

$$F_k(w_k) = \sum_{x \in \mathcal{D}_k} \frac{1}{|D_k|} \mathcal{L}(w_k, x), \tag{2}$$

where w_k denotes the model parameter of user U_k, and $\mathcal{L}(w_k, x)$ is the corresponding loss function. As the data is distributed, it is generally difficult to solve (1) directly. Hence, FL tends to be used by employing an iterative algorithm to train a global model from the users. Specifically, for each round, user U_k calculates the training loss, and then the weights are updated using the gradient descending as

$$v_k \leftarrow w_k - \eta \nabla F_k(w_k), \tag{3}$$

where v_k is the updated model parameter of user U_k and η denotes the learning rate. After that, the updated local models from multiple users are gathered and aggregated at ES.

C. Relay-assisted FEEL

In the considered relay-assisted FEEL, the intermediate relays cooperatively assist the model exchange between users and ES, to extend the coverage and enhance the transmission reliability. Moreover, the relays can perform the operation of aggregation early to cut down the communication cost.

Next, we present in detail the procedure of the FEEL assisted by the relays under the paradigm of FedAvg. Specifically, the global model parameter is initialized to w_0, and then the global model is updated in a number of rounds. At each round, we can divide the model update into the following four steps.

1) User sampling and model broadcast: At this step, ES firstly selects a group of users for each round t. It then broadcasts the global model parameters w^t of the previous round to the selected users with the help of the relays. In particular, ES may uniformly select the user subset $\mathcal{K}$ out of N users without replacement, where $|\mathcal{K}| = K$ is the user number in the user subset $\mathcal{K}$. Note that the uniform selection can be applied to many scenarios where the importance of users is unknown or identical [35]–[37], and it can guarantee the unbiasedness of the model aggregation with full client participation in each round. For other scenarios where the users have different importance, importance-aware scheduling can be adopted to enhance the federated learning performance.

2) Local model update: At this step, user U_k firstly sets the initial local model parameters as $w_k^{t+1} = w^t$, after receiving the global model parameters w^t from ES. Then, user U_k trains its model on its local dataset. Specifically, user U_k conducts E epochs of SGD on its local dataset, where there are totally $e_k = E\frac{|D_k|}{b}$ SGD iterations, and b is the mini-batch size. Therefore, the local model will be updated in a total of e_k times, and in each SGD iteration holds that

$$v_k^{t+1,j+1} \leftarrow v_k^{t+1,j} - \eta_{t+1}\nabla F_k(w_k^{t+1,j};\xi_k), \tag{4}$$

where $j \in \{1,\cdots,e_k\}$ is the local SGD iteration index, and ξ_k is the data batch uniformly chosen from the local dataset D_k.

3) Relay selection and partial aggregation: After finishing the local update, user U_k needs to transmit its updated weight v_k^{t+1} to a selected intermediate relay R_m. Let $\mathcal{J}_m$ denote the user subset uploaded to relay R_m, and $|D_{\mathcal{J}_m}|$ is total the training sample amount in the user subset $\mathcal{J}_m$. After receiving and decoding the local models, relay R_m will aggregate the collected models, where some aggregation method can be applied for the considered relay-assisted federated framework. Without loss of generality, the well-known FedAvg is adopted in this work to aggregate the local trained models, given by

$$w_m^{t+1} = \sum_{\mathrm{U}_k\in\mathcal{J}_m} \frac{|D_k|}{\sum_{\mathrm{U}_k\in\mathcal{J}_m}|D_k|} v_k^{t+1}, \tag{5}$$

where the aggregation at the relay R_m is synchronized, which can help reduce the communication overhead and avoid model staleness, by contrast with the asynchronous federated learning.

Although the synchronous federated learning has the limitation of waiting for slow learners, i.e., stragglers, such limitation can be alleviated through setting a latency threshold to drop out slow users and using proper resource allocation to avoid a long time waiting.

Note that in the above FedAvg, the problem of "objective inconsistency" may arise due to the heterogeneity in the size of local dataset and local SGD iteration among users [38]. This is because the aggregated model will be biased towards the users with more SGD iterations, which eventually affects the federated learning performance. To tackle this problem, we can use the important works [34], [38] and especially the normalized cumulative gradients to replace the FedAvg, given by

$$w_m^{t+1} = w^t + \left(\sum_{\mathrm{U}_k \in \mathcal{J}_m} \frac{|D_k|}{|D_{\mathcal{J}_m}|} e_k \right) \sum_{\mathrm{U}_k \in \mathcal{J}_m} \frac{|D_k|}{|D_{\mathcal{J}_m}|} \frac{v_k^{t+1} - w^t}{e_k}. \tag{6}$$

If not specified, FedAvg will be used for aggregating the local trained models in the subsequent sections.

4) Global Aggregation: At this step, each relay needs to send its aggregated model to the edge server via the second-hop relaying link. After gathering all the models from the relays, the ES can perform the aggregation as

$$w^{t+1} = \sum_{\mathrm{R}_m \in \mathcal{R}} \frac{|D_{\mathcal{J}_m}|}{\sum_{\mathrm{R}_m \in \mathcal{R}} |D_{\mathcal{J}_m}|} w_m^{t+1}. \tag{7}$$

D. Problem Formulation

For the considered relay-assisted FEEL system under latency and bandwidth constraints, we can optimize the system performance through minimizing the global loss function, given by

$$\textbf{P0:} \quad \min \frac{1}{|D|} \sum_{k=1}^{N} \sum_{x \in \mathcal{D}_k} \mathcal{L}(w_k, x). \tag{8}$$

However, obtaining an exact expression for the global loss function of FEEL is generally hard, which causes much difficulty in solving the optimization in problem **P0**. To overcome this difficulty, we turn to perform some analysis on the system performance, as shown in the following section.

III. System performance analysis

A. Latency analysis

The latency is a critical performance metric in the FEEL network, as it determines whether the users can finish the model training and model upload in time or not. When the devices fail to accomplish uploading in time, the effective number of successfully participated users will decrease, causing deterioration in the convergence of federated learning. In the considered relay-assisted FEEL, the latency of each IoT device is related to the computational capability, wireless channel quality, and relay selection. The latency of local training and global aggregation may significantly affect the system training performance. Thus, investigating the latency for the considered relay-assisted FEEL is very important.

The total latency of user U_k is denoted as T_k^{total}, which consists of both the local training latency and the uplink latency. Note that the downlink latency is ignored in this work, as it is generally much smaller than the uplink latency, because the transmit power at the server can be much larger. Specifically, the local training latency T_k^{local} of user U_k is given by

$$T_k^{\text{local}} = \frac{e_k b \rho}{f_k}, \tag{9}$$

where CPU needs ρ cycles to process one sample training, and f_k denotes the computational capability at user U_k. Then, the local trained model needs to be uploaded to ES via the uplink relaying links. In this paper, we perform the relay selection based on the instantaneous CSI of the first-hop relaying links[2]

$$m_k^* = \arg\max_{1 \leq m \leq M} |h_{k,m}|^2, \tag{10}$$

where $h_{k,m}$ is the channel parameter of the link U_k–R_m, and it follows Rayleigh fading with $\mathbb{E}[|h_{k,m}|^2] = \lambda_{k,m}$. The transmission data rate of the link U_k–$\mathrm{R}_{m_k^*}$ is

$$R_{k,m_k^*}^I = B_k^I \log_2\left(1 + \frac{P_k |h_{k,m_k^*}|^2}{\sigma^2}\right), \tag{11}$$

where B_k^I is the allocated bandwidth of the link U_k–$\mathrm{R}_{m_k^*}$, P_k denotes the transmit power at user U_k, and σ^2 denotes the variance of AWGN.

Note that the transmission in (11) employs orthogonal frequency resources among users. If multiple users employ the same frequency resource to communicate simultaneously, the co-channel interference will arise among the users, and the transmission data rate between user U_k and the selected relay $\mathrm{R}_{m_k^*}$ becomes,

$$R_{k,m_k^*}^I = B_{m_k^*}^{II} \log_2\left(1 + \frac{P_k |h_{k,m_k^*}|^2}{\sigma^2 + \sum_{\mathrm{U}_i \in \mathcal{J}_{m_k^*}, i \neq k} P_i |h_{i,m_k^*}|^2}\right), \tag{12}$$

[2] In order to obtain the instantaneous CSI, each user needs to broadcast the transmission request to all relays, and then the users will send some pilot signals to the relays. After that, the relays can estimate the associated channel parameters and execute the relay selection in (10).

where $B^{II}_{m_k^*}$ denotes the bandwidth of the link $\mathrm{R}_{m_k^*}$–ES. From this expression, we can find that the co-channel interference will deteriorate the transmission data rate, and multiple users will have to collaborate or compete in some other domains, such as the power domain in multiuser NOMA systems.

From (11), the transmission latency from user U_k to relay $\mathrm{R}_{m_k^*}$ is given by

$$T^I_{k,m_k^*} = \frac{|L|}{R^I_{k,m_k^*}}, \tag{13}$$

where $|L|$ is the size of the uploaded model. After receiving all the model parameters from the user set $\mathcal{J}_{m_k^*}$, relay $\mathrm{R}_{m_k^*}$ aggregates the local model according to (5). Then, relay $\mathrm{R}_{m_k^*}$ needs to transmit the aggregated model to ES, where the corresponding transmission data rate from relay $\mathrm{R}_{m_k^*}$ to ES is

$$R^{II}_{m_k^*} = B^{II}_{m_k^*} \log_2\left(1 + \frac{P_{m_k^*}|g_{m_k^*}|^2}{\sigma^2}\right), \tag{14}$$

where $P_{m_k^*}$ denotes the transmit power at relay $\mathrm{R}_{m_k^*}$, $g_{m_k^*}$ denotes the instantaneous channel parameter of the link $\mathrm{R}_{m_k^*}$–ES, and it follows Rayleigh fading with $\mathbb{E}[|g_{m_k^*}|^2] = \lambda_{m_k^*}$. In this paper, the relays work in a time-division multiplexing mode, where the dual hops share the same frequency resources, i.e.,

$$B^{II}_{m_k^*} = \sum_{\mathrm{U}_k \in \mathcal{J}_{m_k^*}} B^I_k. \tag{15}$$

From $R^{II}_{m_k^*}$ in (14), the transmission latency from relay $\mathrm{R}_{m_k^*}$ and ES is

$$T^{II}_{m_k^*} = \frac{|L|}{R^{II}_{m_k^*}}. \tag{16}$$

In summary, the total latency of user U_k is

$$T_k^{\text{total}} = T_k^{\text{local}} + T^I_{k,m_k^*} + T^{II}_{m_k^*}. \tag{17}$$

B. Outage Probability Analysis

From the above T_k^{total}, we can start to analyze the outage probability of user U_k. To avoid idle time in the FEEL network, a predetermined latency threshold γ_{th} will be set in practice. The user U_k will be dropped from the federated learning, if the associated latency T_k^{total} is above γ_{th}. Thus, the effective number of users who can successfully participate in federated learning can be given by

$$K_{\text{eff}} = \sum_{k=1}^{K} \mathbb{I}(T_k^{\text{total}} \le \gamma_{th}), \tag{18}$$

where $\mathbb{I}(\cdot)$ denotes the indicator function which returns 1 if the condition is met or 0 otherwise. Accordingly, the expected effective user number is given by

$$\mathbb{E}\left(K_{\text{eff}}\right)=\sum_{k=1}^{K}\Pr[T_k^{\text{total}}\leq\gamma_{th}]=K\left(1-\frac{1}{K}\sum_{k=1}^{K}\Pr[T_k^{\text{total}}>\gamma_{th}]\right). \tag{19}$$

From (19), the system outage probability of the FL is given by

$$P_{out}=\frac{1}{K}\sum_{k=1}^{K}\Pr[T_k^{\text{total}}>\gamma_{th}]=\frac{1}{K}\sum_{k=1}^{K}P_{out,k}, \tag{20}$$

where $P_{out,k}$ is the outage probability of U_k in the process of FL, given by

$$P_{out,k}=\Pr[T_k^{\text{total}}>\gamma_{th}]=\Pr[T_k^{\text{local}}+T_{k,m_k^*}^{I}+T_{m_k^*}^{II}>\gamma_{th}]. \tag{21}$$

To analyze the system outage performance, we need first to derive the outage probability of user U_k. In practice, the local training latency of user U_k can be regarded deterministic, as it is not affected by the stochastic nature of the channels. Hence, we can re-write

$$\begin{aligned}P_{\text{out},k}&=\Pr\left[T_{k,m_k^*}^{I}+T_{m_k^*}^{II}>\gamma_{th}-\frac{d_k}{f_k}\right]=\Pr\left[\frac{|L|}{R_{k,m_k^*}^{I}}+\frac{|L|}{R_{m_k^*}^{II}}>\gamma_{th}-\frac{d_k}{f_k}\right]\\&=\Pr\left[\frac{R_{k,m_k^*}^{I}R_{m_k^*}^{II}}{|L|\left(R_{k,m_k^*}^{I}+R_{m_k^*}^{II}\right)}<\frac{f_k}{\gamma_{th}f_k-d_k}\right],\end{aligned} \tag{22}$$

where $d_k=e_kb\rho$ denotes the CPU cycles needed to finish local training for user U_k.

As deriving an exact closed-form solution to $P_{\text{out},k}$ from (22) is generally hard, we turn to use the inequality of $xy/(x+y)<\min(x,y)$ for positive x and y[3], and then obtain a tight upper bound for the first form in (22) as,

$$\frac{R_{k,m_k^*}^{I}R_{m_k^*}^{II}}{|L|\left(R_{k,m_k^*}^{I}+R_{m_k^*}^{II}\right)}<\frac{1}{|L|}\min(R_{k,m_k^*}^{I},R_{m_k^*}^{II}). \tag{23}$$

Then, substituting (23) into (22), we can obtain the lower bound on the outage probability of user U_k, which can be analytically solved, as shown in Theorem 1,

[3] Note that in this inequality, the approximation error is large when x is equal to y, and the approximation accuracy improves when x differs from y. In general, x is often different from y due to random wireless channels, resulting in a fine approximation accuracy on average. Due to these reasons, the inequality of $xy/(x+y)<\min(x,y)$ is widely used in the existing works such as [39]–[41].

Theorem 1. *A lower bound on the outage probability of user U_k is*

$$P^{lb}_{out,k} = 1 - \exp\left(\frac{1-\exp\left(\frac{f_k|L|\ln 2}{A^{II}_k(\gamma_{th}f_k - d_k)}\right)}{\lambda_{m^*_k}\zeta_{m^*_k}}\right) \cdot \left(1 - \prod_{m=1}^{M}\left(1-\exp\left(\frac{1-\exp\left(\frac{f_k|L|\ln 2}{B^{I}_k(\gamma_{th}f_k - d_k)}\right)}{\lambda_{k,m}\zeta_k}\right)\right)\right). \quad (24)$$

where $\zeta_k = \frac{P_k}{\sigma^2}$ and $\zeta_{m^*_k} = \frac{P_{m^*_k}}{\sigma^2}$ are the transmit SNRs at the user U_k and relay $R_{m^*_k}$, respectively, and A^{II}_k is given by

$$A^{II}_k = \sum_{i=1}^{K-1}\left[\binom{K-1}{i}B^I_k + \binom{K-2}{i-1}(B_{total} - B^I_k)\right]\left(\frac{1}{M}\right)^i\left(1-\frac{1}{M}\right)^{K-i-1} + B^I_k\left(1-\frac{1}{M}\right)^{K-1}, \quad (25)$$

Proof. See Appendix A. ■

Thus, a lower bound on the system outage probability can be obtained in Theorem 2

Theorem 2. *A lower bound on the system outage probability is given by*

$$\begin{aligned} P^{lb}_{out} &= \frac{1}{K}\sum_{k=1}^{K} P^{lb}_{out,k} \\ &= \frac{1}{K}\sum_{k=1}^{K}\left[1-\exp\left(\frac{1-\exp\left(\frac{f_k|L|\ln 2}{A^{II}_k(\gamma_{th}f_k - d_k)}\right)}{\lambda_{m^*_k}\zeta_{m^*_k}}\right)\right. \\ &\quad \left.\times\left(1-\prod_{m=1}^{M}\left(1-\exp\left(\frac{1-\exp\left(\frac{f_k|L|\ln 2}{B^{I}_k(\gamma_{th}f_k - d_k)}\right)}{\lambda_{k,m}\zeta_k}\right)\right)\right)\right]. \end{aligned} \quad (26)$$

Proof. By applying Theorem 1 into (20), the lower bound on the system outage probability can be proved. ■

Note that the above bound contains elementary functions only, which can be easily computed. Therefore, the system outage probability can be easily evaluated in the whole range of SNR.

To obtain more insights on the system design of the relay-assisted FEEL, we use (26) to provide an approximate expression for P^{lb}_{out}, when high SNR region is assumed

$$P^{lb}_{\text{out}} \simeq \frac{1}{K}\sum_{k=1}^{K}\left(1-\left(1-\prod_{m=1}^{M}\frac{\exp\left(\frac{f_k|L|\ln 2}{B^{I}_k(\gamma_{th}f_k - d_k)}\right)-1}{\lambda_{k,m}\zeta_k}\right)\left(1-\frac{\exp\left(\frac{f_k|L|\ln 2}{A^{II}_k(\gamma_{th}f_k - d_k)}\right)-1}{\lambda_{m^*_k}\zeta_{m^*_k}}\right)\right), \quad (27)$$

where the Taylor's series approximation of $\lim\limits_{x\to 0} e^{-x} \simeq 1 - x$ is applied [42]. We further use the approximation of $\lim\limits_{\substack{x\to 0\\ y\to 0}} 1-(1-x)(1-y) \simeq x+y$ and get the asymptotic expression of P_{out}^{lb} for high SNR as

$$\begin{aligned} P_{\text{out}}^{lb} \simeq & \frac{1}{K}\sum_{k=1}^{K}\left(\underbrace{\prod_{m=1}^{M}\left(\exp\left(\frac{f_k|L|\ln 2}{B_k^I\left(\gamma_{th}f_k-d_k\right)}\right)-1\right)\Big/\lambda_{k,m}\zeta_k}_{O_1}+\underbrace{\left(\exp\left(\frac{f_k|L|\ln 2}{A_k^{II}\left(\gamma_{th}f_k-d_k\right)}\right)-1\right)\Big/\lambda_{m_k^*}\zeta_{m_k^*}}_{O_2}\right) \\ & = P_{\text{out}}^{\text{asy}}. \end{aligned} \tag{28}$$

Note that the above asymptotic expression contains two parts, where the first part O_1 depends on the transmission between users and relays, while the second part O_2 depends on the transmission between relays and edge server. From $P_{\text{out}}^{\text{asy}}$, several insights on the FL system can be obtained,

- The first part O_1 decays exponentially with factor M, which indicates that the M intermediate relays can be fully exploited.
- When relay number M is large, the first part O_1 approaches to 0, and the second part O_2 will dominate in the system outage probability, indicating that the transmission between the relays and edge server becomes the system bottleneck.
- The outage performance of the relay-assisted FEEL system improves with a larger $\lambda_{k,m}$ and $\lambda_{m_k^*}$, revealing that a better transmission channel can enhance FL transmission.
- Both O_1 and O_2 are decreasing with respect to B_k^I and A_k^{II} , indicating that a larger bandwidth of user U_k and intermediate relays m_k^* will improve the system outage performance.

C. Convergence Analysis

The convergence of the relay-assisted FEEL is now analyzed, which is of vital importance for the FL training. For this purpose, we first introduce the following assumptions,

Assumption 1: For any user U_k, $F_k(\cdot)$ is μ-strongly convex, i.e., for any w_0 and w_1,

$$F_k(w_1) \geq F_k(w_0) + (w_1 - w_0)^T \nabla F_k(w_0) + \frac{\mu}{2}\|w_1 - w_0\|^2. \tag{29}$$

Assumption 2: For any user U_k, $F_k(\cdot)$ is L-smooth, i.e., for any w_0 and w_1,

$$F_k(w_1) \leq F_k(w_0) + (w_1 - w_0)^T \nabla F_k(w_0) + \frac{L}{2}\|w_1 - w_0\|^2. \tag{30}$$

Assumption 3: For ξ_k uniformly and randomly sampled from the local dataset D_k, the variance of user U_k is bounded for all k by

$$\mathbb{E}\left[\|\nabla F_k(w;\xi_k) - \nabla F_k(w)\|^2\right] \leq \delta_k^2. \tag{31}$$

Assumption 4: For all users, the expected second-order moment of the norm of the stochastic gradient is uniformly bounded by $\mathbb{E}\left[\|\nabla F_k(w;\xi_k)\|^2\right] \leq G^2$.

In addition to the above assumptions, we use the term $\Gamma = F^* - \sum_{k=1}^{N} p_k F_k^*$ to quantify the degree of non-i.i.d, where F^* and F_k^* are the minimum values of F and F_k, respectively. We can find from Γ's definition that the data distribution is i.i.d if $\Gamma = 0$, or non-i.i.d otherwise. Moreover, in order to simplify the analysis, we change the timeline to SGD iterations and assume that all users have the same e SGD iterations in the convergence analysis.

From the above assumptions, the convergence performance of the relay-assisted FEEL can be analyzed, which is presented in Theorem 3.

Theorem 3. *Under Assumption 1-4, with* $\psi = \max\left\{8\frac{L}{\mu}, e\right\}$, *and* $\eta_t = \frac{2}{\mu(\psi+t)}$, *the convergence should satisfy*

$$\mathbb{E}[F(w^T) - F^*] \leq \frac{L}{\mu(\psi+T)}\left[\frac{2}{\mu}\left(\sum_{k=1}^{N} p_k^2\delta_k^2 + 6L\Gamma + 8(e-1)^2G^2 + 4e^2G^2H\right) + \frac{\mu\psi}{2}\left\|w^0 - w^*\right\|^2\right], \tag{32}$$

where $H = \sum_{k=1}^{N} p_k \frac{N-K(1-P_{out})}{K(1-P_{out})}$, *and* w^0 *is the initial value of the global model weights.*

Proof. See Appendix B. ■

From Theorem 3, we can conclude that for the relay-assisted FEEL with partial user participation and user dropout, the terms of $\sum_{k=1}^{N} p_k^2\delta_k^2$, $6L\Gamma$, $8(e-1)^2G^2$, and $4e^2G^2H$ dominate the convergence performance. Specifically, the term $\sum_{k=1}^{N} p_k^2\delta_k^2$ is related to the mini-batch SGD used in the local training, and the term $6L\Gamma$ is related to non-i.i.d data distribution of user data. In particular, the convergence upper bound decreases monotonically with Γ, and when Γ becomes zero, i.e., i.i.d. dataset, the term $6L\Gamma$ can be removed. Moreover, the terms $8(e-1)^2G^2$ and $4e^2G^2H$ are both related to the distributed SGD algorithm and the model aggregation, where the term $4e^2G^2H$ also shows that the effective number of participated users directly affects the convergence upper bound, revealing that a larger outage probability will deteriorate the convergence rate seriously. Thus, it is critical to enhance the convergence performance through reducing the number of users dropped from the FEEL training, by designing a bandwidth allocation scheme for the considered system.

IV. Bandwidth allocation

Inspired by the above convergence results that more users successfully participating in each round's learning process can improve the convergence in Theorem 3, problem **P0** is reformulated as maximizing the successfully participated user number in each round's FL by allocating the wireless bandwidth among users and intermediate relays, given by

$$\textbf{P1:} \max_{\{B_k^I, B_m^{II} | \mathrm{U}_k \in \mathcal{U}, \mathrm{R}_m \in \mathcal{R}\}} K_{\text{eff}} = \sum_{k=1}^{K} \mathbb{I}(T_k^{\text{total}} \le \gamma_{th}) \tag{33a}$$

$$\text{s.t.} \sum_{\mathrm{R}_m \in \mathcal{R}} B_m^{II} \le B_{\text{total}}, \tag{33b}$$

$$\sum_{\mathrm{U}_k \in \mathcal{J}_m} B_k^I = B_m^{II}, \tag{33c}$$

where (33b) and (33c) are the bandwidth constraints at the relays and users, respectively. These two bandwidth constraints also indicate that multiple users will collaborate or compete with each other in the frequency domain, which can be found in many application scenarios where the users employ some orthogonal frequency resources to communicate, such as OFDMA systems. On the other hand, if the users employ the same frequency resource to communicate simultaneously, co-channel interference will arise, and multiple users have to collaborate or compete in some other domains, such as the power domain in multiuser NOMA systems. In this case, the proposed framework of performance analysis and system optimization in this paper is still applicable, and the results in this work can serve as a useful benchmark for the federated learning with multiuser interference, which can help obtain some insights on the system design.

In the following, the optimization problem is solved by exploiting the instantaneous or statistical CSI, where flexible choices can be provided for the system optimization.

A. *Instantaneous Bandwidth Allocation*

For the instantaneous bandwidth allocation method, the edge server needs to make bandwidth allocation decision at each time slot, so that the instantaneous bandwidth allocation tends to be used in the system which is sensitive to the performance of communication and training. Due to the indicator function and the coupling of constraints (33b) and (33c), the problem **P1** is hard to be directly solved. Thus, we propose to solve this problem by dividing it into two sub-problems: minimizing the total bandwidth required for the selected users and choosing some users to be dropped out from the FEEL process. Specifically, for the first sub-problem, we relax the problem

P1 by removing the bandwidth constraint (33b), so that all the relays can be allocated by the required bandwidth, in order to support the selected users to successfully participate in FEEL process. The first sub-problem can be given by

$$\textbf{P2:} \quad \min_{\{B_k^I, \alpha_{k,m} | \mathrm{U}_k \in \mathcal{U}, \mathrm{R}_m \in \mathcal{R}\}} \sum_{\mathrm{R}_m \in \mathcal{R}} B_m^{II} \tag{34a}$$

$$\text{s.t. } T_k^{\text{local}} + \frac{|L|}{\alpha_{k,m} B_m^{II} r_{k,m}^I} + \frac{|L|}{B_m^{II} r_m^{II}} \leq \gamma_{th}, \forall \mathrm{U}_k \in \mathcal{U}, \tag{34b}$$

$$\sum_{\mathrm{U}_k \in \mathcal{J}_m} \alpha_{k,m} = 1, \tag{34c}$$

$$0 \leq \alpha_{k,m} \leq 1, \tag{34d}$$

where $r_{k,m}^I = \log_2\left(1 + \frac{P_k |h_{k,m}|^2}{\sigma^2}\right)$, $r_m^{II} = \log_2\left(1 + \frac{P_m |g_m|^2}{\sigma^2}\right)$, and $\alpha_{k,m}$ is the bandwidth allocation ratio from relay R_m to user U_k, which satisfies $0 \leq \alpha_{k,m} \leq 1$ and $\sum_{\mathrm{U}_k \in \mathcal{J}_m} \alpha_{k,m} = 1$. Constraint (34b) guarantees that all users can successfully participate in the training process. Constraints (34c) and (34d) are the reformulation of (33c) using $B_k^I = \alpha_{k,m} B_m^{II}$ as the bandwidth allocated to user U_k from relay R_m. We can find that the optimal solution of **P2** should satisfy the conditions given in Theorem 4,

Theorem 4. *For relay R_m, the optimal $B_m^{II^*}$ and $\alpha_{k,m}^*$ to solve problem **P2** should satisfy*

$$\begin{cases} T_k^{local} + \dfrac{|L|}{\alpha_{k,m}^* B_m^{II^*} r_{k,m}^I} + \dfrac{|L|}{B_m^{II^*} r_m^{II}} = \gamma_{th}, & (35a) \\ \displaystyle\sum_{U_k \in \mathcal{J}_m} \alpha_{k,m}^* = 1, & (35b) \\ 0 \leq \alpha_{k,m}^* \leq 1, & (35c) \\ B_m^{II} \geq 0. & (35d) \end{cases}$$

Proof. See Appendix C. ■

From Theorem 4, we can observe that there is one and only one solution to (35) because of the monotonicity and non-trivial value of $\alpha_{k,m}^*$ and $B_m^{II^*}$. Moreover, with a given $B_m^{II^*}$, we can get the optimal value of $\alpha_{k,m}$ as

$$\alpha_{k,m}^* = \frac{r_m^{II} |L|}{B_m^{II^*} (\gamma_{th} - T_k^{\text{local}}) r_{k,m}^I r_m^{II} - r_{k,m}^I |L|}. \tag{36}$$

With (36), we can obtain a numerical value of $B_m^{II^*}$ by using an efficient searching algorithm based on the bisection method, as shown in Algorithm 1. In particular, we start the search with

Algorithm 1: Bisection search of $B_m^{II^*}$ and $\alpha_{k,m}^*$

```
Input $B_{\text{total}}$, $\mathcal{J}_m$ ;
$B_{\text{lower}} = 0$, $B_{\text{upper}} = B_{\text{total}}$;
while $B_{lower} < B_{upper}$ do
    $B_{\text{mid}} = (B_{\text{lower}} + B_{\text{upper}})/2$;
    For $\mathrm{U}_k \in \mathcal{J}_m$, calculate the bandwidth ratio $\alpha_{k,m}$ according to (36) with $B_{\text{mid}}$;
    if $\sum_{U_k \in \mathcal{J}_m} \alpha_{k,m} < 1$ then
        $B_{\text{lower}} = B_{\text{mid}}$;
    else if $\sum_{U_k \in \mathcal{J}_m} \alpha_{k,m} > 1$ then
        $B_{\text{upper}} = B_{\text{mid}}$;
    else if $\sum_{U_k \in \mathcal{J}_m} \alpha_{k,m} = 1$ then
        $B_m^{II^*} = B_{\text{mid}}, \alpha_{k,m}^* = \alpha_{k,m}, \mathrm{U}_k \in \mathcal{J}_m$;
        break;
    end
end
Output $B_m^{II^*}$, $\{\alpha_{k,m}^* | \mathrm{U}_k \in \mathcal{J}_m\}$
```

the middle point B_{mid} of an initial range $[B_{\text{lower}}, B_{\text{upper}}]$. With B_{mid} as the bandwidth allocated to relay R_m, we then calculate $\alpha_{k,m}$ for each user $\mathrm{U}_k \in \mathcal{J}_m$ and sum up all $\alpha_{k,m}$. By comparing $\sum_{\mathrm{U}_k \in \mathcal{J}_m} \alpha_{k,m}^*$ with 1, we can halve the search region with $B_{\text{upper}} = B_{\text{mid}}$ if $\sum_{\mathrm{U}_k \in \mathcal{J}_m} \alpha_{k,m} > 1$, or halve the search region with $B_{\text{lower}} = B_{\text{mid}}$ otherwise. The search process will continue until the constraint (35b) is satisfied, which finally outputs the optimal $\alpha_{k,m}$ for $\mathrm{U}_k \in \mathcal{J}_m$ and B_m^{II}.

We proceed to solve the second sub-problem when the total bandwidth needed exceeds the system total bandwidth, i.e., $\sum_{\mathrm{R}_m \in \mathcal{R}} B_m^{II} > B_{\text{total}}$. In this case, the participating users should be adjusted and certain users have to be dropped out to satisfy the bandwidth constraint (33b). Here, a greedy algorithm is utilized to solve the second sub-problem. Specifically, the user with the largest $\alpha_{k,m} B_m^{II}$, i.e., the user occupies the largest bandwidth, will be dropped out from the FEEL process. After removing the firstly dropped out user, we continue to solve problem **P2** until the constraint $\sum_{\mathrm{R}_m \in \mathcal{R}} B_m^{II} \leq B_{\text{total}}$ is satisfied. In this way, we finally solve problem **P1** with the instantaneous CSI. The greedy based bandwidth allocation algorithm with the instantaneous CSI

Algorithm 2: Greedy based bandwidth allocation algorithm

```
Input $\mathcal{U}$, $\mathcal{R}$, $\mathcal{J}_m$, $B_{\text{total}}$;
For $\mathrm{R}_m \in \mathcal{R}$, Solve $B_m^{II^*}$, $\alpha^*_{k,m}$ using Algorithm 1;
while $\sum_{R_m \in \mathcal{R}} B_m^{II^*} > B_{total}$ do
    $\mathrm{U}_k{}', \mathrm{R}_m{}' = \arg\max_{\mathrm{U}_k \in \mathcal{U}, \mathrm{R}_m \in \mathcal{R}} \alpha^*_{k,m} B_m^{II^*}$;
    $B^I_{k'} = 0$;
    $\mathcal{U} = \mathcal{U} \setminus \mathrm{U}_k{}', \mathcal{J}_{m'} \setminus \mathrm{U}_k{}'$;
    Solve $B_m^{II^*}$, $\alpha^*_{k,m}$ using Algorithm 1 with $\mathcal{U}$ and $\mathcal{J}_m, \mathrm{R}_m \in \mathcal{R}$;
end
$B_m^{II} = B_m^{II^*}, B_k^I = \alpha^*_{k,m} B_m^{II^*}, \mathrm{U}_k \in \mathcal{J}_m, \mathrm{R}_m \in \mathcal{R}$;
Output $\{B_k^I, B_m^{II} | \mathrm{U}_k \in \mathcal{U}, \mathrm{R}_m \in \mathcal{R}\}$
```

is summarized in Algorithm 2.

B. Statistical Bandwidth Allocation

Besides the above instantaneous BA method, we also provide a statistical bandwidth allocation, which is performed once for many time slots and applicable to the system that is sensitive to the computational complexity of bandwidth allocation at the price of some performance deterioration compared with the instantaneous bandwidth allocation. In this case, we turn problem **P1** into optimizing the statistical expectation of the successfully participated user number in each round's FL, given by

$$\textbf{P3:} \max_{\{B_k^I, B_m^{II} | \mathrm{U}_k \in \mathcal{U}, \mathrm{R}_m \in \mathcal{R}\}} \mathbb{E}\left(K_{\text{eff}}\right) = K\left(1 - P_{out}\right) \tag{37a}$$

$$s.t. \sum_{\mathrm{R}_m \in \mathcal{R}} B_m^{II} \le B_{\text{total}}, \tag{37b}$$

$$\sum_{\mathrm{U}_k \in \mathcal{J}_m} B_k^I = B_m^{II}. \tag{37c}$$

As obtaining an exact analytical expression for P_{out} is hard, we turn to employ the derived lower bound P_{out}^{lb} to help approximate the expectation of the number of users successfully participating in FEEL. Thus, we can reformulate **P3** into **P4**, given by

$$\textbf{P4:} \max_{\{B_k^I, B_m^{II} | \mathrm{U}_k \in \mathcal{U}, \mathrm{R}_m \in \mathcal{R}\}} K(1 - P_{out}^{lb}) \tag{38a}$$

$$s.t. \sum_{\mathrm{R}_m \in \mathcal{R}} B_m^{II} \leq B_{\text{total}}, \tag{38b}$$

$$\sum_{\mathrm{U}_k \in \mathcal{J}_m} B_k^I = B_m^{II}. \tag{38c}$$

As problem **P4** is hard to be directly solved, we use the particle swarm optimization (PSO) to solve problem **P4**, which is an intelligent algorithm using a set of "particles" to search for an approximate solution. In PSO, there are I particles, and each particle i has three associated vectors: the velocity v_i, the position p_i, and the best position $pbest_i$. Specifically, p_i is a K-dimension vector denoting a feasible solution of bandwidth allocation, where $p_i = \{B_k^I | \mathrm{U}_k \in \mathcal{K}\}$, v_i is a K-dimension vector of bandwidth variation, where $v_i = \{\Delta B_k^I | \mathrm{U}_k \in \mathcal{K}\}$, and $pbest_i$ is a K-dimension vector of the best solution to the optimization problem for particle i. Moreover, there is a global vector $gbest$ used to denote the best solution among all the particles. All the position vectors are potential solutions of the optimization problem evaluated by the fitness function $F_{\text{fitness}}(\cdot)$, measured by $K(1 - P_{out}^{lb})$.

For particle i at iteration t, its velocity is updated as

$$v_i^t = \omega v_i^{t-1} + \varphi_1 \rho_1 \left(pbest_i^{t-1} - p_i^{t-1}\right) + \varphi_2 \rho_2 \left(gbest^{t-1} - p_i^{t-1}\right), \tag{39}$$

where ω denotes the inertia weight of the previous velocity, φ_1 and φ_2 are two acceleration coefficients, and ρ_1 and ρ_2 are two random variables uniformly distributed in [0,1]. The position of particle i is updated as

$$p_i^t = p_i^{t-1} + v_i^t. \tag{40}$$

After E times of iteration of velocity and position updates, the $gbest$ obtained from I particles can be regarded as a feasible solution to problem **P4**. The PSO based bandwidth allocation algorithm with the statistical CSI is summarized in Algorithm 3.

V. Simulation results

In this part, some analytical and simulation results are presented to validate the proposed studies in this paper. In particular, the basic setting of these simulations is introduced, along with some baselines methods used for comparison. We then present some simulations with the

Algorithm 3: PSO based bandwidth allocation algorithm

```
Input $\mathcal{U}$, $\mathcal{R}$, $\mathcal{J}_m$, $B_{\text{total}}$, $I$, $T$, $\omega$, $\varphi_1$, $\varphi_2$;
Initialize Create $I$ particles randomly;
for $t = 1$ to $T$ do
    for $i = 1$ to $I$ do
        Update $\boldsymbol{v}_i^t$ by (39), and update $\boldsymbol{p}_i^t$ by (40);
        if $F_{\textit{fitness}}\left(\boldsymbol{p}_i^t\right) \leq F_{\textit{fitness}}\left(\boldsymbol{pbest}_i^t\right)$ then
            $\boldsymbol{pbest}_i^t = \boldsymbol{p}_i^t$;
        end
        if $F_{\textit{fitness}}\left(\boldsymbol{p}_i^t\right) \leq F_{\textit{fitness}}\left(\boldsymbol{gbest}^t\right)$ then
            $\boldsymbol{gbest}^t = \boldsymbol{p}_i^t$;
        end
    end
end
$B_m^{II} = \sum_{\mathrm{U}_k \in \mathcal{J}_m} B_k^I, \mathrm{R}_m \in \mathcal{R}$;
Output $\{B_k^I, B_m^{II} | \mathrm{U}_k \in \mathcal{U}, \mathrm{R}_m \in \mathcal{R}\}$
```

purpose of verifying the derived analysis on the system outage performance. Further, we conduct some more simulations to validate instantaneous and statistical bandwidth allocation schemes.

A. Simulation Settings

The simulations are performed in the considered relay-assisted FEEL system with a total of 200 users. If not specified, for all simulations, there are 500 communication rounds in total, and there are 10 selected users for each communication round. The channels follow Rayleigh flat fading, where the average channel gain of the link U_k–R_m is set to $\lambda_{k,m} = (100 + k)/200$, and the average channel gain between the relays and ES is set to 2. The transmit power at each user and each relay are set to 0.1W and 0.5W, respectively. The computational capability of each user is 1.5×10^7cycle/second. In addition, for the PSO based bandwidth allocation algorithm, we use 30 particles and 50 iterations to search for a feasible solution, where the inertia weight of the previous velocity ω is 0.5 and the two acceleration coefficients φ_1 and φ_2 are both 0.4.

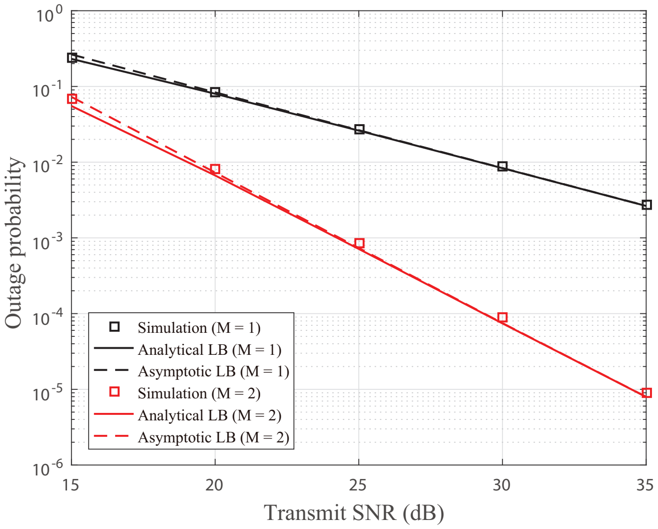

Fig. 2. Outage probability of the considered relay-assisted FEEL system versus the transmit SNR.

In practice, for the FL task, the Fashion-MNIST dataset is used to perform a classification task, where 60000 training and 10000 test samples are utilized. There are 10 classes of fashion pictures in the training samples, and the number of training samples allocated for each user is uniformly distributed as $|D_k| \in \mathcal{U}(200, 400)$. For the non-i.i.d setting of the Fashion-MNIST dataset, each user is assigned with 2 labels in its local training samples. As to the learning network, we use a CNN composed of two 3×3 convolution layers, each followed by a batch normalization layer and a 2×2 max pooling layer, two fully connected layers, a drop out layer between the two fully connected layers, and a soft output layer. For the training of the CNN network, we use the CrossEntropyLoss as the loss function with $\eta = 0.001$, $b = 30$, and $E = 3$.

To verify the effectiveness of the proposed instantaneous and statistical bandwidth allocation schemes, we compare with some baseline methods abbreviated as follows,

- **Ideal FEEL:** There is no bandwidth or latency constraint so that all the selected users can successfully take part in the learning process.
- **Uniform allocation (UA):** ES performs the uniform bandwidth allocation for all users selected in each communication round.
- **Uniform allocation without partial aggregation (UA-wo-PA):** ES performs the uniform bandwidth allocation for all users selected in each communication round, and the users upload the model via the selected relay without partial aggregation.

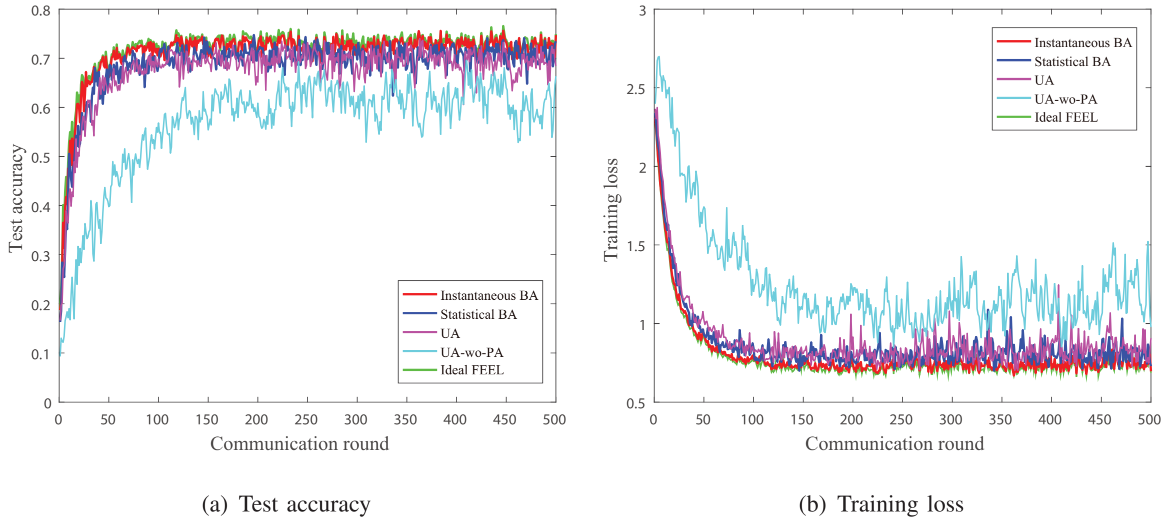

(a) Test accuracy

(b) Training loss

Fig. 3. Test accuracy and training loss through aggregating the trained models.

B. Outage Performance Simulation

Fig. 2 depicts the simulated, analytical and asymptotic outage probabilities for the relay-assisted FEEL under UA method versus the transmit SNR, where the transmit SNR of each user ranges from 15dB to 35dB, the transmit SNR of each relay is ten times that of the user, and the total bandwidth of the system is 50MHz. Observing from Fig. 2, we can find that the analytical lower bound fits well with the simulated one, and the asymptotic lower bound converges to the analytical one with high SNR, which shows the correctness of the derived analytical and asymptotic expressions of the system outage probability. Moreover, all the system outage results get improved when SNR becomes larger, as a larger transmit power at users and relays can achieve a reduced latency in the model upload, thus improving the system outage performance. Further to this, it is found that the system outage probability improves with a larger M, as more relays can help increase the spatial diversity of the wireless links between users and relays.

C. Federated Learning Performance Simulation

Fig. 3(a) and Fig. 3(b) illustrate the test accuracy and training loss of the aforementioned BA schemes, where $B_{\text{total}} = 60$MHz, and $\gamma_{th} = 1.2$s. We can observe from Fig. 3(a) and Fig. 3(b) that both the test accuracy and training loss of all BA schemes converge with the increasing communication round. Moreover, the UA-wo-PA performs the worst, because without partial aggregation, more models need to be uploaded through the second hop. Further, the

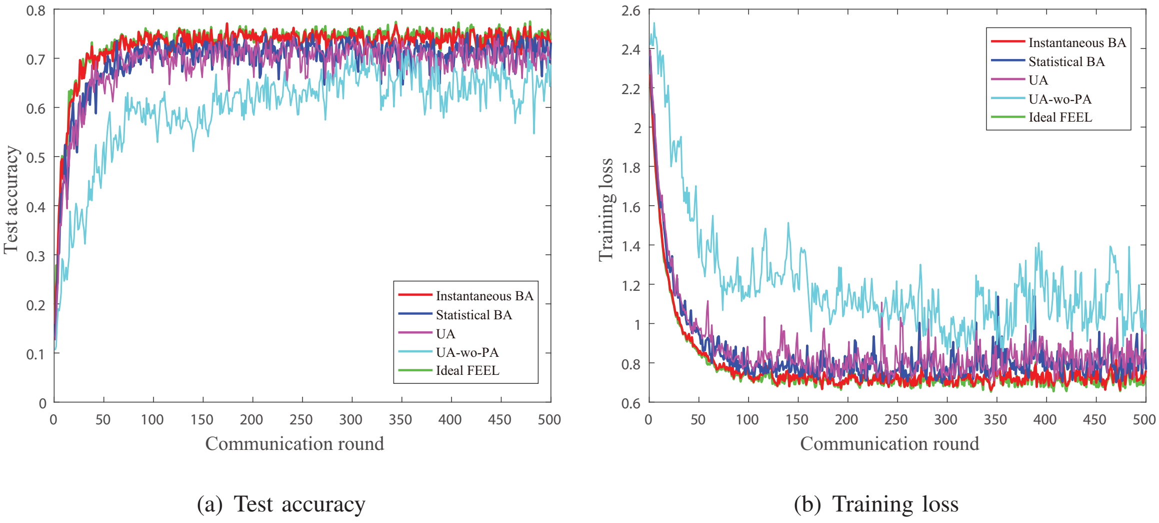

(a) Test accuracy

(b) Training loss

Fig. 4. Test accuracy and training loss through aggregating the normalized cumulative gradients.

proposed instantaneous and statistical bandwidth allocation schemes outperform UA, showing the effectiveness of the two bandwidth allocation schemes. Furthermore, the instantaneous bandwidth allocation scheme can achieve a better near-optimal convergence rate and test accuracy than the statistical bandwidth allocation scheme, indicating that the instantaneous CSI can help maximize the number of users who can successfully participate in FL at each round more effectively.

Fig. 4(a) and Fig. 4(b) show the test accuracy and training loss of the aforementioned BA schemes versus the communication round through aggregating the normalized cumulative gradients, where $B_{\text{total}} = 60$MHz, and $\gamma_{th} = 1.2$s. We can observe that the proposed instantaneous and statistical BA schemes outperform UA, proving the effectiveness of the two bandwidth allocation schemes when aggregating the normalized cumulative gradients. Moreover, aggregating the normalized cumulative gradients can provide a better performance with an improved test accuracy of 1%-1.5% than simply aggregating the trained models in the FedAvg, which demonstrates that the problem of "objective inconsistency" caused by different SGD iterations would deteriorate the federated learning performance, and using normalized cumulative gradients in the aggregation can help solve the inconsistency problem and enhance the system performance.

Fig. 5 is provided to show the test accuracy of the several BA schemes versus γ_{th}, where $M \in \{1, 2\}$ and the system latency threshold varies from 0.8s to 1.8s. We can observe that for all the aforementioned schemes except the ideal FEEL one, the test accuracy gets improved with a larger system threshold, as a larger threshold can allow more users successfully to participate

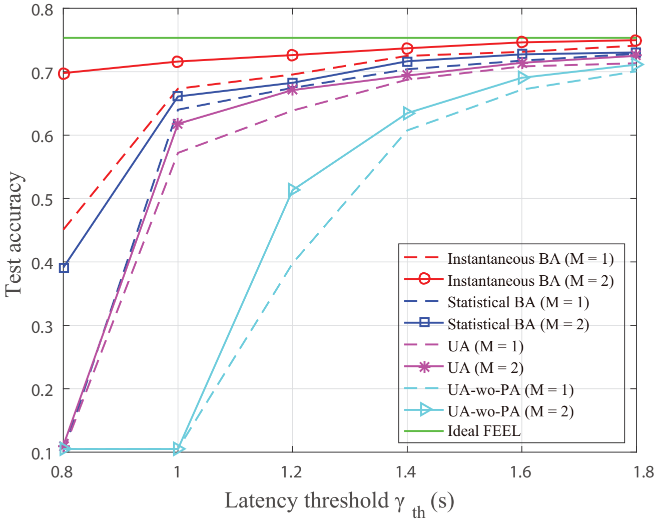

Fig. 5. Test accuracy of the several BA schemes versus γ_{th}.

in FEEL. Moreover, for all the aforementioned schemes, the performances with two relays are better than those with only one relay, since more relays can help improve the model transmission rate. In further, the UA and UA-wo-PA schemes have a lower test accuracy than the instantaneous and statistical BA schemes. In particular, when the latency threshold is low, the relay-assisted FEEL system using the UA and UA-wo-PA schemes can not even train an effective model. This is because that only very few users can successfully participate in FEEL under those schemes. However, the proposed instantaneous and statistical BA schemes can achieve sufficiently good performance for various latency thresholds, which proves that instantaneous and statistical BA schemes can provide a feasible bandwidth allocation strategy for the relay-assisted FEEL.

Fig. 6 shows the impact of B_{total} on the test accuracy of the several bandwidth allocation schemes, where the relay number $M \in \{1, 2\}$, $\gamma_{th} = 1.2$s, and B_{total} varies from 50MHz to 100MHz. The test accuracy improvements are observed for all the aforementioned schemes except the ideal FEEL one, as B_{total} increases, indicating that a larger bandwidth can help increase the transmission rate of the models. Moreover, we can see that with the number of relays increasing from 1 to 2, all the bandwidth allocation schemes get improved because more relays can help enhance the outage performance and allow more users successfully participate in FEEL. In further, the proposed instantaneous and statistical BA schemes outperform the other bandwidth allocation schemes for a wide range of B_{total}, and they can achieve almost the same accuracy as the ideal FEEL. These results further verify the proposed bandwidth allocation

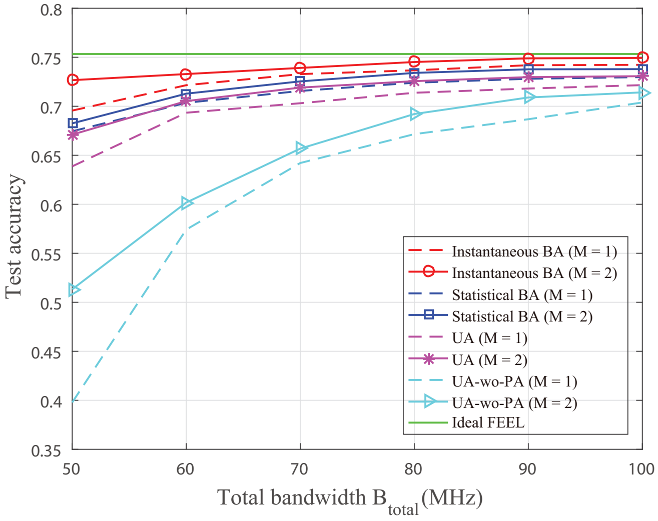

Fig. 6. Test accuracy of the several BA schemes versus B_{total}.

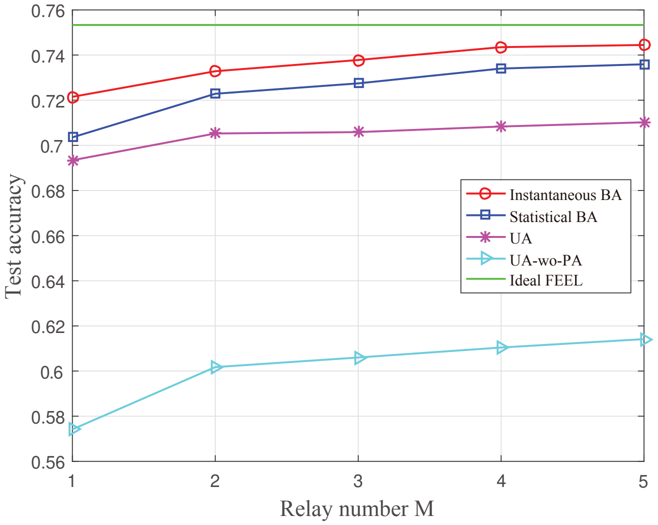

Fig. 7. Test accuracy of the several BA schemes versus M.

schemes.

In Fig. 7, the influence of the relay number on the test accuracy of the several BA schemes is studied, where the relay number varies from 1 to 5, $B_{total} = 60$MHz, and $\gamma_{th} = 1.2$s. We can observe from this figure that all the bandwidth allocation schemes are improved with a larger M, as spatial diversity and better transmission connections can be provided for model uploading. Moreover, the proposed instantaneous and statistical BA schemes are superior to the other bandwidth allocation schemes, including UA and the UA-wo-PA schemes. In particular, when there are four relays in the network, the proposed instantaneous and statistical BA schemes can achieve a better test accuracy, at least 5.1% and 3.8% higher than that of the UA and UA-wo-PA schemes. These results indicate that the proposed instantaneous and statistical BA schemes can efficiently exploit multiple relays and improve the performance of the relay-assisted FEEL.

VI. Conclusion

In this article, a relay-assisted FEEL system was studied under latency and bandwidth constraints, where we evaluated the system performance by deriving analytical and asymptotic expressions of the system outage probability and the convergence analysis. In order to improve the system performance, we optimized the relay-assisted FEEL network through allocating the wireless bandwidth among users and relays. Specifically, we proposed two bandwidth allocation schemes to maximize the successfully participated user number in each round's federated learning. Finally, some simulations were demonstrated to verify the instantaneous and statistical bandwidth allocation schemes. The simulation results showed that the proposed instantaneous and statistical BA schemes could outperform the conventional UA and UA-wo-PA schemes, and achieve almost the same performance as the conventional federated learning without latency and bandwidth constraints. In future works, we will study the federated learning with multiuser interference for the considered system, where the proposed framework of performance analysis and system optimization in this paper will be applied.

References

[1] W. Saad, M. Bennis, and M. Chen, "A vision of 6G wireless systems: Applications, trends, technologies, and open research problems," *IEEE Netw.*, vol. 34, no. 3, pp. 134–142, 2020.

[2] S. Deng, H. Zhao, W. Fang, J. Yin, S. Dustdar, and A. Y. Zomaya, "Edge intelligence: The confluence of edge computing and artificial intelligence," *IEEE Internet Things J.*, vol. 7, no. 8, pp. 7457–7469, 2020.

[3] X. Wang, Y. Han, C. Wang, Q. Zhao, X. Chen, and M. Chen, "In-edge AI: Intelligentizing mobile edge computing, caching and communication by federated learning," *IEEE Netw.*, vol. 33, no. 5, pp. 156–165, 2019.

[4] W. Zhou, J. Xia, and F. Zhou, "Profit maximization for cache-enabled vehicular mobile edge computing networks," *to appear in IEEE Trans. Veh. Technol.*, pp. 1–6, 2023.

[5] B. McMahan, E. Moore, D. Ramage, S. Hampson, and B. A. y Arcas, "Communication-efficient learning of deep networks from decentralized data," in *Proc. AISTATS*, vol. 54, 2017, pp. 1273–1282.

[6] S. Wang, T. Tuor, T. Salonidis, K. K. Leung, C. Makaya, T. He, and K. Chan, "Adaptive federated learning in resource constrained edge computing systems," *IEEE J. Sel. Areas Commun.*, vol. 37, no. 6, pp. 1205–1221, 2019.

[7] W. Shi, S. Zhou, Z. Niu, M. Jiang, and L. Geng, "Joint device scheduling and resource allocation for latency constrained wireless federated learning," *IEEE Trans. Wirel. Commun.*, vol. 20, no. 1, pp. 453–467, 2021.

[8] A. Hammoud, H. Otrok, A. Mourad, and Z. Dziong, "On demand fog federations for horizontal federated learning in iov," *IEEE Trans. Netw. Serv. Manag.*, vol. 19, no. 3, pp. 3062–3075, 2022.

[9] Z. Zhao, C. Feng, W. Hong, J. Jiang, C. Jia, T. Q. S. Quek, and M. Peng, "Federated learning with non-iid data in wireless networks," *IEEE Trans. Wirel. Commun.*, vol. 21, no. 3, pp. 1927–1942, 2022.

[10] Y. Zhan, J. Zhang, Z. Hong, L. Wu, P. Li, and S. Guo, "A survey of incentive mechanism design for federated learning," *IEEE Trans. Emerg. Top. Comput.*, vol. 10, no. 2, pp. 1035–1044, 2022.

[11] M. Wazzeh, H. Ould-Slimane, C. Talhi, A. Mourad, and M. Guizani, "Privacy-preserving continuous authentication for mobile and iot systems using warmup-based federated learning," *IEEE Netw.*, pp. 1–7, 2022.

[12] G. Zhu, D. Liu, Y. Du, C. You, J. Zhang, and K. Huang, "Toward an intelligent edge: Wireless communication meets machine learning," *IEEE Commun. Mag.*, vol. 58, no. 1, pp. 19–25, 2020.

[13] W. Zhou, L. Fan, F. Zhou, F. Li, X. Lei, W. Xu, and A. Nallanathan, "Priority-aware resource scheduling for UAV-mounted mobile edge computing networks," *to appear in IEEE Trans. Veh. Technol.*, pp. 1–6, 2023.

[14] L. Xiao, Y. Ding, J. Huang, S. Liu, Y. Tang, and H. Dai, "UAV anti-jamming video transmissions with QoE guarantee: A reinforcement learning-based approach," *IEEE Trans. Commun.*, vol. 69, no. 9, pp. 5933–5947, 2021.

[15] L. Xiao, X. Lu, T. Xu, X. Wan, W. Ji, and Y. Zhang, "Reinforcement learning-based mobile offloading for edge computing against jamming and interference," *IEEE Trans. Commun.*, vol. 68, no. 10, pp. 6114–6126, 2020.

[16] R. Yu and P. Li, "Toward resource-efficient federated learning in mobile edge computing," *IEEE Netw.*, vol. 35, no. 1, pp. 148–155, 2021.

[17] X. Huang, P. Li, R. Yu, Y. Wu, K. Xie, and S. Xie, "Fedparking: A federated learning based parking space estimation with parked vehicle assisted edge computing," *IEEE Trans. Veh. Technol.*, vol. 70, no. 9, pp. 9355–9368, 2021.

[18] J. Ren, Y. He, D. Wen, G. Yu, K. Huang, and D. Guo, "Scheduling for cellular federated edge learning with importance and channel awareness," *IEEE Trans. Wirel. Commun.*, vol. 19, no. 11, pp. 7690–7703, 2020.

[19] X. Cao, G. Zhu, J. Xu, Z. Wang, and S. Cui, "Optimized power control design for over-the-air federated edge learning," *IEEE J. Sel. Areas Commun.*, vol. 40, no. 1, pp. 342–358, 2022.

[20] H. Sun, X. Ma, and R. Q. Hu, "Adaptive federated learning with gradient compression in uplink NOMA," *IEEE Trans. Veh. Technol.*, vol. 69, no. 12, pp. 16 325–16 329, 2020.

[21] H. Yang, J. Zhao, Z. Xiong, K. Lam, S. Sun, and L. Xiao, "Privacy-preserving federated learning for UAV-enabled networks: Learning-based joint scheduling and resource management," *IEEE J. Sel. Areas Commun.*, vol. 39, no. 10, pp. 3144–3159, 2021.

[22] S. Zheng, C. Shen, and X. Chen, "Design and analysis of uplink and downlink communications for federated learning," *IEEE J. Sel. Areas Commun.*, vol. 39, no. 7, pp. 2150–2167, 2021.

[23] M. Salehi and E. Hossain, "Federated learning in unreliable and resource-constrained cellular wireless networks," *IEEE Trans. Commun.*, vol. 69, no. 8, pp. 5136–5151, 2021.

[24] J. Xu and H. Wang, "Client selection and bandwidth allocation in wireless federated learning networks: A long-term perspective," *IEEE Trans. Wirel. Commun.*, vol. 20, no. 2, pp. 1188–1200, 2021.

[25] S. Tang, L. Chen, K. He, J. Xia, L. Fan, and A. Nallanathan, "Computational intelligence and deep learning for next-generation edge-enabled industrial IoT," *IEEE Trans. Netw. Sci. Eng.*, vol. PP, no. 99, pp. 1–12, 2023.

[26] Z. Zhao, J. Xia, L. Fan, X. Lei, G. K. Karagiannidis, and A. Nallanathan, "System optimization of federated learning networks with a constrained latency," *IEEE Trans. Veh. Technol.*, vol. 71, no. 1, pp. 1095–1100, 2022.

[27] Y. Wang, Y. Xu, Q. Shi, and T. Chang, "Quantized federated learning under transmission delay and outage constraints," *IEEE J. Sel. Areas Commun.*, vol. 40, no. 1, pp. 323–341, 2022.

[28] Q. Bie, Y. Liu, Y. Wang, X. Zhao, and X. Y. Zhang, “Deployment optimization of reconfigurable intelligent surface for relay systems,” *IEEE Trans. Green Commun. Netw.*, vol. 6, no. 1, pp. 221–233, 2022.

[29] J. Xia, L. Fan, W. Xu, X. Lei, X. Chen, G. K. Karagiannidis, and A. Nallanathan, “Secure cache-aided multi-relay networks in the presence of multiple eavesdroppers,” *IEEE Trans. Commun.*, vol. 67, no. 11, pp. 7672–7685, 2019.

[30] X. Li, R. Fan, H. Hu, N. Zhang, X. Chen, and A. Meng, “Energy-efficient resource allocation for mobile edge computing with multiple relays,” *IEEE Internet Things J.*, vol. 9, no. 13, pp. 10 732–10 750, 2022.

[31] S. Feng, D. Niyato, P. Wang, D. I. Kim, and Y.-C. Liang, “Joint service pricing and cooperative relay communication for federated learning,” in *2019 International Conference on Internet of Things (iThings)*, 2019, pp. 815–820.

[32] Z. Lin, H. Liu, and Y. A. Zhang, “Relay-assisted cooperative federated learning,” *IEEE Trans. Wirel. Commun.*, vol. 21, no. 9, pp. 7148–7164, 2022.

[33] Z. Qu, S. Guo, H. Wang, B. Ye, Y. Wang, A. Y. Zomaya, and B. Tang, “Partial synchronization to accelerate federated learning over relay-assisted edge networks,” *IEEE Trans. Mob. Comput.*, vol. 21, no. 12, pp. 4502–4516, 2022.

[34] S. Hosseinalipour, S. Wang, N. Michelusi, V. Aggarwal, C. G. Brinton, D. J. Love, and M. Chiang, “Parallel successive learning for dynamic distributed model training over heterogeneous wireless networks,” *CoRR*, vol. abs/2202.02947, 2022.

[35] C. Shen, J. Xu, S. Zheng, and X. Chen, “Resource rationing for wireless federated learning: Concept, benefits, and challenges,” *IEEE Commun. Mag.*, vol. 59, no. 5, pp. 82–87, 2021.

[36] H. Yang, M. Fang, and J. Liu, “Achieving linear speedup with partial worker participation in non-iid federated learning,” in *9th International Conference on Learning Representations, ICLR 2021*, 2021.

[37] S. P. Karimireddy, S. Kale, M. Mohri, S. J. Reddi, S. U. Stich, and A. T. Suresh, “SCAFFOLD: Stochastic controlled averaging for on-device federated learning,” *CoRR*, vol. abs/1910.06378, 2019.

[38] J. Wang, Q. Liu, H. Liang, G. Joshi, and H. V. Poor, “Tackling the objective inconsistency problem in heterogeneous federated optimization,” in *NeurIPS 2020*, 2020.

[39] J. Tong and C. Zhong, “Full-duplex two-way AF relaying systems with imperfect interference cancellation in Nakagami-m fading channels,” *Sci. China Inf. Sci.*, vol. 64, no. 8, 2021.

[40] O. Waqar, H. Tabassum, and R. Adve, “Secure beamforming and ergodic secrecy rate analysis for amplify-and-forward relay networks with wireless powered jammer,” *IEEE Trans. Veh. Technol.*, vol. 70, no. 4, pp. 3908–3913, 2021.

[41] L. Fan, X. Lei, T. Q. Duong, M. Elkashlan, and G. K. Karagiannidis, “Secure multiuser communications in multiple amplify-and-forward relay networks,” *IEEE Trans. Commun.*, vol. 62, no. 9, pp. 3299–3310, 2014.

[42] I. S. Gradshteyn and I. M. Ryzhik, *Table of Integrals, Series, and Products*, 7th ed. San Diego, CA: Academic, 2007.

[43] X. Li, K. Huang, W. Yang, S. Wang, and Z. Zhang, “On the convergence of fedavg on non-iid data,” in *ICLR*, 2020.

APPENDIX A
PROOF OF THEOREM 1

To prove Theorem 1, we substitute (23) into (22), and then the lower bound of $P_{\text{out},k}$ is,

$$
\begin{aligned}
P_{\text{out},k} \geq & \Pr\left(\frac{1}{|L|}\min(R^{I}_{k,m_k^*}, R^{II}_{m_k^*}) < \frac{1}{\gamma_{th} - T_k^{\text{local}}}\right) = 1 - \Pr\left(\frac{1}{|L|}\min(R^{I}_{k,m_k^*}, R^{II}_{m_k^*}) \geq \frac{1}{\gamma_{th} - T_k^{\text{local}}}\right) \\
=& 1 - \left(1 - \Pr\left(R^{I}_{k,m_k^*} < \frac{|L|}{\gamma_{th} - T_k^{\text{local}}}\right)\right)\left(1 - \Pr\left(R^{II}_{m_k^*} < \frac{|L|}{\gamma_{th} - T_k^{\text{local}}}\right)\right). \qquad \text{(A.1)}
\end{aligned}
$$

After some manipulations, we can further have,

$$
\begin{aligned}
P_{\text{out},k} \geq & 1 - \left(1 - \Pr\left(|h_{k,m_k^*}|^2 < \frac{2^{\frac{|L|}{B_k^I\left(\gamma_{th}-T_k^{\text{local}}\right)}}-1}{\zeta_k}\right)\right)\left(1 - \Pr\left(|g_{m_k^*}|^2 < \frac{2^{\frac{|L|}{B_{m_k^*}^{II}\left(\gamma_{th}-T_k^{\text{local}}\right)}}-1}{\zeta_{m_k^*}}\right)\right)\\
= & 1 - \left(1 - \prod_{m=1}^{M} \Pr\left(|h_{k,m}|^2 < \frac{2^{\frac{|L|}{B_k^I\left(\gamma_{th}-T_k^{\text{local}}\right)}}-1}{\zeta_k}\right)\right)\left(1 - \Pr\left(|g_{m_k^*}|^2 < \frac{2^{\frac{|L|}{B_{m_k^*}^{II}\left(\gamma_{th}-T_k^{\text{local}}\right)}}-1}{\zeta_{m_k^*}}\right)\right).
\end{aligned}
\tag{A.2}
$$

As $|h_{k,m}|^2$ and $|g_{m_k^*}|^2$ are exponentially distributed with $\mathbb{E}[|h_{k,m}|^2] = \lambda_{k,m}$ and $\mathbb{E}[|g_{m_k^*}|^2] = \lambda_{m_k^*}$, the analytical lower bound on $P_{\text{out},k}$ is written as,

$$
P_{\text{out},k} \geq 1 - \left(1 - \prod_{m=1}^{M}\left(1 - \exp\left(\frac{1-\exp\left(\frac{|L|\ln 2}{B_k^I\left(\gamma_{th}-T_k^{\text{local}}\right)}\right)}{\lambda_{k,m}\zeta_k}\right)\right)\right)\mathbb{E}\left[\exp\left(\frac{1-\exp\left(\frac{|L|}{B_{m_k^*}^{II}\left(\gamma_{th}-T_k^{\text{local}}\right)}\right)}{\lambda_{m_k^*}\zeta_{m_k^*}}\right)\right].
\tag{A.3}
$$

We can observe from (A.3) that $\exp\left(\left(1-\exp\left(\frac{|L|}{B_{m_k^*}^{II}\left(\gamma_{th}-T_k^{\text{local}}\right)}\right)\right)/\lambda_{m_k^*}\zeta_{m_k^*}\right)$ is concave for a positive $B_{m_k^*}^{II}$. By using Jensen's inequality, we have

$$
P_{\text{out},k} \geq 1 - \left(1 - \prod_{m=1}^{M}\left(1 - \exp\left(\frac{1-\exp\left(\frac{|L|\ln 2}{B_k^I\left(\gamma_{th}-T_k^{\text{local}}\right)}\right)}{\lambda_{k,m}\zeta_k}\right)\right)\right)\exp\left(\frac{1-\exp\left(\frac{|L|\ln 2}{A_k^{II}\left(\gamma_{th}-T_k^{\text{local}}\right)}\right)}{\lambda_{m_k^*}\zeta_{m_k^*}}\right),
\tag{A.4}
$$

where A_k^{II} is the expected bandwidth of the relay selected by user U_k, given in (25). In this way, we have proven Theorem 1.

Appendix B
Proof of Theorem 3

Before proving Theorem 3, we first present some notations and lemmas to facilitate the proof. Specifically, we define $\bar{w}^t = \sum_{k=1}^{N} p_k w_k^t$ and $\bar{v}^t = \sum_{k=1}^{N} p_k v_k^t$, where $p_k = \frac{|D_k|}{|D|}$. Then, we present two preliminary lemmas used for the proof.

Lemma 1. *Using (7) and taking the system outage into account, we can write the aggregated global model at time t as*

$$
w^{t+1} = w^{t+1-e} + \sum_{k=1}^{N} \frac{\mathbb{I}(k \in \mathcal{K}, T_k^{total} \leq \gamma_{th})|D_k|}{\sum_{k\in\mathcal{K}} \mathbb{I}(T_k^{total} \leq \gamma_{th})|D_k|}(v_k^{t+1} - w^{t+1-e}).
\tag{B.1}
$$

Lemma 2. *The two-stage aggregation in the relay-assisted FEEL is unbiased, i.e.,* $\mathbb{E}[\bar{w}^t] = \bar{v}^t$.

Proof. Using (B.1), we have

$$\begin{aligned}\mathbb{E}[\bar{w}^t] =&\mathbb{E}\left[w^{t-e} + \sum_{k=1}^{N} \frac{\mathbb{I}(k \in \mathcal{K}, T_k^{\text{total}} \leq \gamma_{th})|D_k|}{\sum_{k \in \mathcal{K}} \mathbb{I}(T_k^{\text{total}} \leq \gamma_{th})|D_k|}(v_k^t - w^{t-e})\right] \\ =&w^{t-e} + \sum_{k=1}^{N} \frac{|D_k|}{\frac{K}{N}(1-P_{out})|D|} \cdot \mathbb{E}\left[\mathbb{I}(k \in \mathcal{K}, T_k^{\text{total}} \leq \gamma_{th})\right](v_k^t - w^{t-e}) \\ =&w^{t-e} + \sum_{k=1}^{N} p_k(v_k^t - w^{t-e}) = \sum_{k=1}^{N} p_k v_k^t = \bar{v}^t. \end{aligned} \tag{B.2}$$

■

Then, we proceed with the proof of Theorem 3 by looking into assumption 2 of Sec.III-C, where we have

$$\mathbb{E}[F(w^T) - F^*] \leq \frac{L}{2}\mathbb{E}\left[\left\|\bar{w}^{t+1} - w^*\right\|^2\right]. \tag{B.3}$$

Thus, we only need to bound $\mathbb{E}\left[\left\|\bar{w}^{t+1} - w^*\right\|^2\right]$ for the proof, which can be further written as

$$\begin{aligned}&\mathbb{E}\left[\left\|\bar{w}^{t+1} - w^*\right\|^2\right] = \mathbb{E}\left[\left\|\bar{w}^{t+1} - \bar{v}^{t+1} + \bar{v}^{t+1} - w^*\right\|^2\right] \\ &= \underbrace{\mathbb{E}\left[\left\|\bar{w}^{t+1} - \bar{v}^{t+1}\right\|^2\right]}_{Q_1} + \underbrace{\mathbb{E}\left[\left\|\bar{v}^{t+1} - w^*\right\|^2\right]}_{Q_2} + \underbrace{2\mathbb{E}\left[\left(\bar{w}^{t+1} - \bar{v}^{t+1}\right)^T\left(\bar{v}^{t+1} - w^*\right)\right]}_{Q_3}. \end{aligned} \tag{B.4}$$

Next, we bound $\mathbb{E}\left[\left\|\bar{w}^{t+1} - w^*\right\|^2\right]$ part by part. Specifically, for the first part Q_1, we have

$$\begin{aligned}Q_1 =&\mathbb{E}\left[\left\|\bar{w}^{t+1} - \bar{v}^{t+1}\right\|^2\right] \\ =&\mathbb{E}\left[\left\|w^{t-e} + \sum_{k=1}^{N} \frac{\mathbb{I}(k \in \mathcal{K}, T_k^{\text{total}} \leq \gamma_{th})|D_k|}{\sum_{k \in \mathcal{K}} \mathbb{I}(T_k^{\text{total}} \leq \gamma_{th})|D_k|}(v_k^{t+1} - w^{t+1-e}) - \sum_{k=1}^{N} p_k v_k^{t+1}\right\|^2\right] \\ =&\mathbb{E}\left[\left\|w^{t-e} + \sum_{k=1}^{N} p_k \frac{\mathbb{I}(k \in \mathcal{K}, T_k^{\text{total}} \leq \gamma_{th})}{\frac{K}{N}(1-P_{out})}(v_k^{t+1} - w^{t+1-e}) - \sum_{k=1}^{N} p_k\left(v_k^{t+1} - w^{t+1-e}\right)\right\|^2\right] \\ =&\mathbb{E}\left[\left\|\sum_{k=1}^{N} p_k\left(\frac{N \cdot \mathbb{I}(k \in \mathcal{K}, T_k^{\text{total}} \leq \gamma_{th})}{K(1-P_{out})} - 1\right) \cdot (v_k^{t+1} - w^{t+1-e})\right\|^2\right]. \end{aligned} \tag{B.5}$$

Using the convexity of the second-order norm, we further have

$$\begin{aligned}Q_1 \leq& \mathbb{E}\left[\sum_{k=1}^{N} p_k\left\|\left(\frac{N \cdot \mathbb{I}(k \in \mathcal{K}, T_k^{\text{total}} \leq \gamma_{th})}{K(1-P_{out})} - 1\right) \cdot (v_k^{t+1} - w^{t+1-e})\right\|^2\right] \\ =& \sum_{k=1}^{N} p_k \frac{N - K(1-P_{out})}{K(1-P_{out})} \cdot \mathbb{E}\left[\left\|v_k^{t+1} - w^{t+1-e}\right\|^2\right]. \end{aligned} \tag{B.6}$$

We can write $\mathbb{E}\left[\left\|v_k^{t+1} - w^{t+1-e}\right\|^2\right]$ in (B.6) as

$$\mathbb{E}\left[\left\|v_k^{t+1} - w^{t+1-e}\right\|^2\right] = \mathbb{E}\left[\left\|\sum_{i=t+1-e}^{t} \eta_i \nabla F_k(w_k^i;\xi_k^i)\right\|^2\right] \leq \mathbb{E}\left[e\cdot\sum_{i=t+1-e}^{t}\left\|\eta_i \nabla F_k(w_k^i;\xi_k^i)\right\|^2\right]$$

$$\leq \mathbb{E}\left[\eta_{t+1-e}^2 e\cdot\sum_{t}^{i=t+1-e}\left\|\nabla F_k(w_k^i;\xi_k^i)\right\|^2\right] \leq \eta_{t+1-e}^2 e^2 G^2 \leq 4\eta_{t+1}^2 e^2 G^2 \leq 4\eta_t^2 e^2 G^2, \tag{B.7}$$

where we use the Cauchy-Schwarz inequality for the first inequality, and we assume that η_t is non-increasing with respect to t and $\eta_t \leq 2\eta_{t+E}$ to derive other inequalities. Then, we can bound the first part Q_1 as

$$Q_1 = \mathbb{E}\left[\left\|\bar{w}^{t+1} - w^*\right\|^2\right] \leq \sum_{k=1}^{N} p_k \frac{N - K(1-P_{out})}{K(1-P_{out})}\cdot 4\eta_t^2 e^2 G^2. \tag{B.8}$$

For the second part Q_2, its bound can be found in [43], which can still hold for this paper. Thus, according to [43], we have that for any round t, if we choose $\psi = \max\left\{8\frac{L}{\mu}, e\right\}$ and $\eta_t = \frac{2}{\mu(\psi+t)}$, the second part Q_2 is bounded as

$$Q_2 = \mathbb{E}\left[\left\|\bar{v}^{t+1} - w^*\right\|^2\right] \leq (1-\mu\eta_t)\mathbb{E}\left[\left\|\bar{w}^{t} - w^*\right\|^2\right] + \eta_t^2\left(\sum_{k=1}^{N} p_k^2\delta_k^2 + 6L\Gamma + 8(e-1)^2G^2\right). \tag{B.9}$$

For the third part Q_3, we can derive from Lemma 2 that Q_3 equals to 0 due to the unbiasedness of $\bar{w}^{t+1}$. By summarizing the above three parts, we have that, for any round t, $\mathbb{E}\left[\left\|\bar{w}^{t+1} - w^*\right\|^2\right]$ is bounded as

$$\mathbb{E}\left[\left\|\bar{w}^{t+1} - w^*\right\|^2\right] \leq (1-\mu\eta_t)\mathbb{E}\left[\left\|\bar{w}^{t} - w^*\right\|^2\right] + \eta_t^2\left(\sum_{k=1}^{N} p_k^2\delta_k^2 + 6L\Gamma + 8(e-1)^2G^2 + 4e^2G^2H\right), \tag{B.10}$$

in which $H = \sum_{k=1}^{N} p_k \frac{N-K(1-P_{out})}{K(1-P_{out})}$. For brevity, we rewrite (B.10) as

$$\Delta_{t+1} \leq (1-\mu\eta_t)\Delta_t + C, \tag{B.11}$$

where $\Delta_{t+1} = \mathbb{E}\left[\left\|\bar{w}^{t+1} - w^*\right\|^2\right]$ and

$$C = \sum_{k=1}^{N} p_k^2\delta_k^2 + 6L\Gamma + 8(e-1)^2G^2 + 4e^2G^2H. \tag{B.12}$$

Then, we use the recurrence method to prove that $\Delta_t \le \frac{v}{\psi+t}$, where $v = \max\left\{\psi\Delta_0, \frac{\beta^2 C}{\mu\beta-1}\right\}$. First, for $t=0$, we have $\Delta_0 \le \frac{v}{\psi+0} \le \Delta_0$. For $t>0$, we have

$$\Delta_{t+1} \le (1-\mu\eta_t)\Delta_t + \eta_t^2 C = \frac{t+\psi-1}{(t+\psi)^2}v + \left[\frac{\beta^2 C}{(t+\psi)^2} - \frac{\mu\beta-1}{(t+\psi)^2}v\right] \le \frac{1}{t+\psi+1}. \qquad \text{(B.13)}$$

Therefore, we have

$$\begin{aligned}\mathbb{E}[F(w^T)-F^*] &\le \frac{L}{2}\mathbb{E}\left[\left\|\bar{w}^{t+1}-w^*\right\|^2\right]\\ &\le \frac{L}{\mu(\psi+T)}\left[\frac{2}{\mu}\left(\sum_{k=1}^{N} p_k^2\delta_k^2 + 6L\Gamma + 8(e-1)^2G^2 + 4e^2G^2H\right) + \frac{\mu\psi}{2}\left\|w^0-w^*\right\|^2\right]. \qquad \text{(B.14)}\end{aligned}$$

In this way, we have proven Theorem 3.

Appendix C

Proof of Theorem 4

To prove Theorem 4, we start from $\alpha_{k,m} > 0$ and $B_m^{II} > 0$ to have

$$\frac{\mathrm{d}R_{k,m}^{I}}{\mathrm{d}\alpha_{k,m}} = \frac{\mathrm{d}}{\mathrm{d}\alpha_{k,m}}\left(\alpha_{k,m}B_m^{II}\log_2\left(1+\frac{P_k|h_{k,m}|^2}{\sigma^2}\right)\right) = B_m^{II}\log_2\left(1+\frac{P_k|h_{k,m}|^2}{\sigma^2}\right) > 0, \qquad \text{(C.1)}$$

and

$$\frac{\mathrm{d}R_{k,m}^{I}}{\mathrm{d}B_m^{II}} = \frac{\mathrm{d}}{\mathrm{d}B_m^{II}}\left(\alpha_{k,m}B_m^{II}\log_2\left(1+\frac{P_k|h_{k,m}|^2}{\sigma^2}\right)\right) = \alpha_{k,m}\log_2\left(1+\frac{P_k|h_{k,m}|^2}{\sigma^2}\right) > 0, \qquad \text{(C.2)}$$

we can see from (C.1) and (C.2) that $R_{k,m}^{I}$ monotonically increases with $\alpha_{k,m}$ and B_m^{II}. Therefore, for $\alpha_{k,m} > 0$, and $B_m^{II} > 0$, we have that $T_{k,m}^{I}$ and T_m^{II} monotonically decrease with $\alpha_{k,m}$ and B_m^{II}. Moreover, the system latency is determined by the slowest user. Therefore, we can achieve the optimal solution of **P2** if and only if: 1) all of the bandwidth B_m^{II} is allocated (i.e., $\sum_{k\in\mathcal{J}_m}\alpha_{k,m} = 1$) and 2) all selected users have the same total latency of γ_{th} (i.e., $T_k^{\text{total}} = T_k^{\text{local}} + T_{k,m}^{I} + T_m^{II} = \gamma_{th}$). So the optimal solution can be given by

$$\begin{cases} T_k^{\text{total}} + \frac{|L|}{\alpha_{k,m}^* B_m^{II^*} r_{k,m}^{I}} + \frac{|L|}{B_m^{II^*} r_m^{II}} = \gamma_{th}, \\ \sum_{\mathrm{U}_k\in\mathcal{J}_m}\alpha_{k,m}^* = 1, \\ 0 \le \alpha_{k,m}^* \le 1, \\ B_m^{II} \ge 0. \end{cases} \qquad \text{(C.3)}$$

Because of the monotonicity and non-trivial value of $\alpha_{k,m}^*$ and $B_m^{II^*}$, there is one and only one solution to (C.3), which finishes the proof of Theorem 4.